THE GEOLOGICAL SOCIETY OF AMERICA®

A Method for Developing Regional Road-Fill Failure Hazard Assessments Using GIS and Virtual Fieldwork

ROBERT J. SAS, JR.

LEONARD S. SKLAR

Department of Geosciences, San Francisco State University, 1600 Holloway Avenue, San Francisco, CA 94112

L. SCOTT EATON

Department of Geology and Environmental Sciences, James Madison University, MSC 6903, Harrisonburg, VA 22807

JERRY DAVIS

Department of Geography and Human Environmental Studies, San Francisco State University, 1600 Holloway Avenue, San Francisco, CA 94112

Key Terms: ***Models, Probability, Landslides, Management, Geomorphology, GIS***

ABSTRACT

Road-fill failure is a common and potentially catastrophic hazard on mountainous roads. Land managers need methods for assessing road-fill failure hazards that minimize time in the field and that use readily available data. We developed a probabilistic hazard assessment method using virtual fieldwork and LiDAR-derived slope distributions over a 97-km length of the Blue Ridge Parkway in North Carolina. The locations of arc-shaped pavement cracks and previous road-fill failures were mapped using field-verified VisiData video reconnaissance, and the slopes surrounding failed-or-cracked sites were extracted from a digital elevation model and compared to uncracked portions of road. The site-median slopes of the failed-or-cracked sites and uncracked sites are normally distributed and significantly different ($P < 0.01$) from one another. This observation provides the basis for a probabilistic, hazard assessment model that uses the site-median slope of a 30-m–diameter buffer to categorize currently uncracked sites as either stable or at risk of road-fill failure during future high-intensity rainfall events.

INTRODUCTION

Road-fill failures initiated during heavy rainfall are a common and very serious management problem for transportation networks in mountainous terrain (e.g., Douglas, 1967; Larsen and Parks, 1997; and Wemple et al., 2001). These failures can threaten human life, are costly to repair, and result in protracted road closures that disrupt normal travel for months. Fill failures can also produce debris flows (Collins, 2008), causing accelerated surface erosion and sedimentation in watersheds, which can perturb the natural environment to the extent that some habitats are not recoverable (Furniss et al., 1991). Fill-type failures are a concern for all mountainous roads, particularly aging roadways in National Parks and forests, many of which were constructed in the 1930s and 1940s. Commonly, progressive road-fill failures are only mitigated when collapse appears imminent, or they are repaired after catastrophic failure, and little attention is given to predicting the locations of potential future failures over a larger region. Although several analytical models exist for predicting sediment yield from forested roads (Elliot and Tysdal, 1999; Elliot and Lewis, 2000), few physically based, analytical models that use site-specific field information are capable of predicting the initiation of failures themselves, especially on modified slopes. Most existing models are physically based and calculate a factor of safety based on variables that are either held constant over the entire landscape (e.g., angle of internal friction, bulk density) (Dietrich et al., 1995) or have limited site specificity (Pack et al., 1998); none of these models were designed to analyze modified slopes. A rational probabilistic model is a practical compromise between infinite slope/factor of safety and probabilistic modeling approaches (Haneberg, 2004), but this model requires expertise to apply effectively. Other similar analyses have required intensive field data collection efforts (Rollerson et

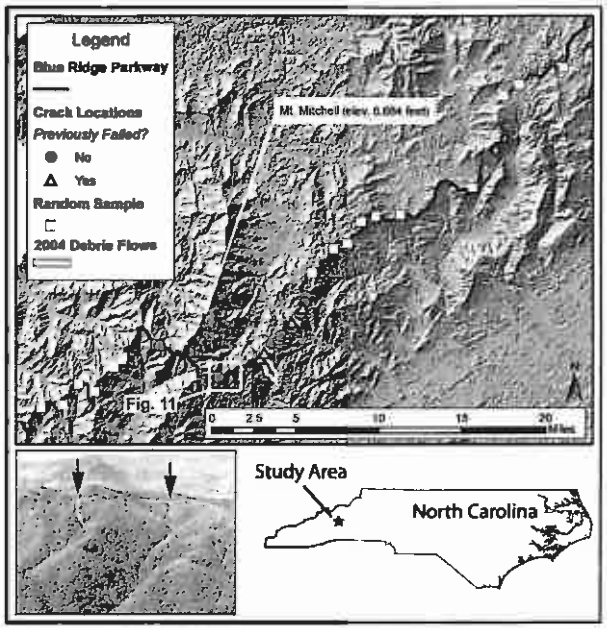

Figure 1. The study area is a 97-km portion of the Blue Ridge Parkway (BRP) in North Carolina. Inset photo: Arrows point to September 2004 road failures that resulted in debris flows shown on map.

al., 2002), which are often impractical for managers of roadways with extensive fill slopes.

Here we describe a method to quantify the topographic attributes associated with road failure along the Blue Ridge Parkway in North Carolina (BRP) (Latham, 2006; Collins, 2008) (Figure 1). With the aid of Geographic Information System (GIS) tools and modeling, and by using a combination of virtual fieldwork using VisiData software, field verification, and a high-resolution digital elevation model (DEM), we were able to develop a model to provide a probabilistic hazard assessment of fill-slope stability along the BRP. Since quantitative analysis of topographic attributes is of increasing importance in terms of understanding how natural landscapes function (e.g., Stock and Dietrich, 2006), it follows that these concepts be applied to modified landscapes as well. Slope angle is arguably the most fundamental topographic attribute and is readily quantifiable from a DEM, though dependent on spatial resolution. Field measurements can rarely capture topographic attributes at the scale and resolution necessary for a regional assessment of hill-slope hazards (Dietrich and Montgomery, 1998). However, arc-shaped pavement cracks (hereafter referred to as "cracks") observed in the field are a reliable indicator of gravity-driven failure of the fill material and have been used as a field constraint for fill-slope stability along the BRP (Collins, 2008).

In the following sections we present the regional setting of the BRP, describe the data collection and analysis methods, derive a simple probabilistic model for assessing road-fill failure potential, and discuss application of the model to practical road management decision making.

REGIONAL SETTING

The BRP spans approximately 755 highway kilometers of rugged terrain in the Blue Ridge physiographic province of the southern Appalachians and links the Shenandoah National Park in Virginia with the Great Smoky Mountains National Park in North Carolina. Our study area is between mileposts 310 and 370 (Linville Falls to Craggy Gardens, respectively), northeast of Asheville, NC (Figure 1). The project site lies within the Ashe Metamorphic Suite and Tallulah Falls Formation, dominantly consisting of mica-schist and gneiss (North Carolina Geological Survey, 1985; Merschat et al., 2006). Surficial soils are described as loose stone with some admixture of Porters loam (Federal Highway Administration, 2004).

In 2004 there were more hurricanes in the Atlantic basin than usual, with 15 named storms and six Category 3 hurricanes on the Saffir-Simpson Scale. Two of those storms impacted the southern end of the BRP between the dates of September 6 and September 19, dropping as much as 584+ mm and 254+ mm of rainfall from Hurricanes Frances and Ivan, respectively (Beven, 2004). The climate of Asheville is humid temperate, with 1,194 mm of precipitation fairly evenly distributed throughout the year, and 381 mm of snow (National Climate Data Center, 2000). Despite the fact that Hurricane Ivan was ranked as the ninth most intense Atlantic hurricane on record (as well as the only Category 5 storm of 2004), it was Frances that persisted for an extended period over the southern Appalachians, resulting in higher rainfall totals and five road-fill failures in the study area (Figure 2). Near the center of the study area is Mount Mitchell, the highest peak east of the Mississippi River, with an elevation of 2,037 m. Thus, the orography of the region has an important influence on weather systems and rainfall initiation of landslides (Wooten et al., 2008).

DATA COLLECTION AND ANALYSIS METHODS

We used two basic types of data, digital video and field-verified road condition data, provided by VisiData, and topographic data derived from airborne laser swath mapping or LiDAR.

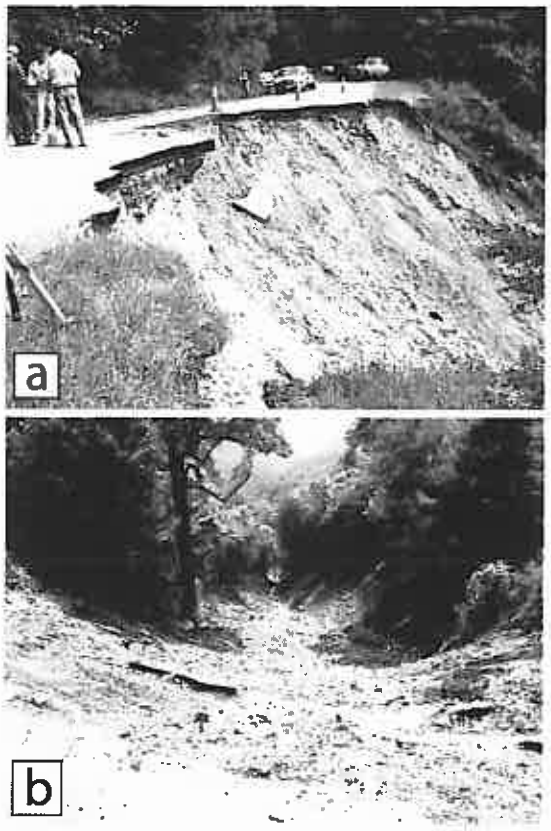

Figure 2. (a) Initiation site of road-fill failure (milepost 348.8) and (b) downslope impacts from debris flow. Arc-shaped pavement crack at initiation site was evident months prior to failure in September 2004. Photos courtesy of the Federal Highway Administration.

The VisiData program visualizes digital video and quantitative road inventory data (e.g., pavement condition, locations of signs) for out-of-the-field reconnaissance and is an interface to perform virtual fieldwork because all data are geographically positioned. VisiData provides the user with a software interface for analyzing archived records of pavement conditions, including 160°–forward-view digital video, mosaic photographs of the pavement surface, observed drainage structures, and a spectral analysis of pavement surface conditions. The data are collected by technicians operating a vehicle, called the automated road analyzer (ARAN), outfitted with various cameras, sensors, and a Global Positioning System (GPS) receiver.

Fortunately, the initial VisiData reconnaissance of the pavement of BRP was made 3 months in advance of Hurricanes Frances and Ivan. In June 2004, an instrumented truck traveling the full length of the BRP collected visual data of the viewscape and of the competency and conditions of the pavement. For our purposes, the most significant resource provided by

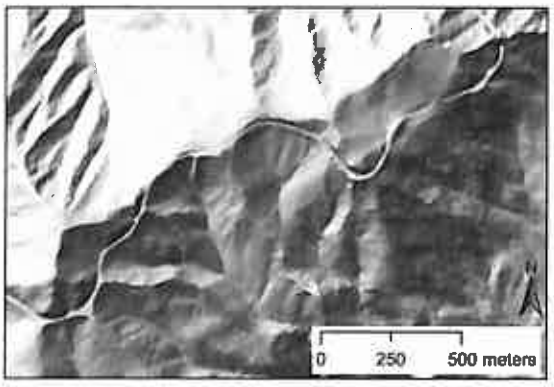

Figure 3. The 6-m resolution LiDAR-derived digital elevation data used in this study show in detail the topographic presence of the Blue Ridge Parkway, as demonstrated by this hillshade model for a portion of the study area.

VisiData was the seamless digital video. The digital video captures travel lanes, drainage structures, and traffic safety controls and provides good visualization of immediately adjacent upslopes and downslopes. In order to quantify the reliability of the VisiData interpretations, we investigated on foot each highway kilometer in our 97-km study area. Twenty-one sites of past or current pavement arcuate cracking were documented during the field reconnaissance (Figure 1), 19 of which were evident in the VisiData. Each site was identified via GPS coordinates, followed by a documentation of roadway conditions. We found >90 percent agreement of the virtual fieldwork with our on-foot observations. Data on the crack topology, dimensions, drainage structures, and other pavement conditions were recorded. VisiData is currently available for nearly all federally managed, paved roadways (Jim Amenta, Federal Highway Administration, pers. comm.) and is being implemented by numerous other agencies, both within the United States and internationally.

Data from a VisiData, GPS-delineated road polyline were combined with a 6-m–resolution DEM (Figure 3) for topographic analysis. The LiDAR-derived elevation data used in this study (available for download; North Carolina Department of Transportation, 2007) were collected in April 2007 after the 2004 failures occurred. We consider these data representative of the prefailure road slope morphology because the repair of the 2004 failures sites involved restoring the prefailure fill-slope roadway topography.

Using tools in ArcGIS 9.1 (Environmental Systems Research Institute, Redlands, CA), we extracted slopes from within analysis buffers 30 m in radius that extend along the entire roadway (Figure 4; total of 130,000 grid cells). Included in this data set are cells

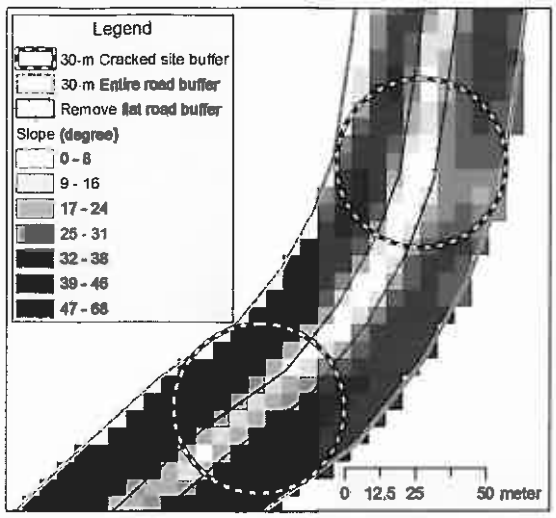

Figure 4. Figure shows segment of slope raster output from Geographic Information System (GIS). Analysis buffers with 30-m radius to extract slope distributions are shown as bold, dashed lines for failed-or-cracked sites and as a gray line for the entire uncracked road. Hatched lines are 6-m-radius analysis buffers used to remove slope distribution of flat, paved road.

occupied by the paved roadway, which has a nearly flat surface. To avoid skewing the slope distribution toward the low slope tail, we used a narrow (6-m radius) buffer to extract slopes from the paved roadway and subtracted this distribution from the 30-m buffer data set (Figure 5). Several bridges and tunnels present in the study area were removed from this analysis since their engineered stability is unrelated to fill-slope stability.

To characterize the slope distribution representative of the failed-or-cracked sites, we extracted slopes from 30-m-radius circular buffers centered on the surveyed location of the cracks for each of the 21 failed-or-cracked sites. Each circular buffer contains ~70 cells. As illustrated in Figure 4, we used a 6-m-

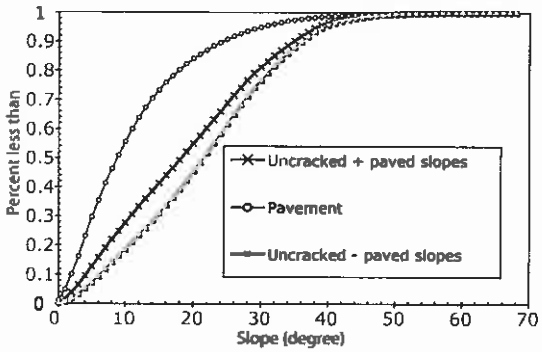

Figure 5. Plot shows a cumulative, normalized distribution of cracked slopes plus paved slopes from entire roadway in study area. Paved slopes and cracked minus paved slopes are also shown.

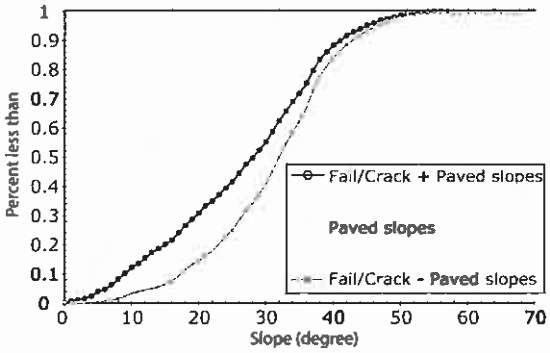

Figure 6. Plot shows a cumulative, normalized distribution of lumped failed-or-cracked slopes plus paved slopes from individual sites in study area. Paved slopes and failed-or-cracked minus paved slopes are also shown.

radius buffer through each site to extract the slope values associated with the paved roadway (~18 cells per site) and then subtracted these values from the failed-or-cracked slope distributions for each site. Figure 6 shows the distributions of all slope values for all 21 sites lumped together, with and without the paved roadway data. Finally, to fully separate the failed-or-cracked and uncracked slope distributions, we subtracted the lumped failed-or-cracked slope values from the entire roadway slope set to obtain two distributions representative of the two distinct site populations, shown in Figure 7.

PROBABILISTIC MODEL DEVELOPMENT

For our topographic analysis, we assume sites can be divided into two populations: unlikely to fail (stable) and likely to fail eventually (potentially unstable). Potentially unstable sites can be subdivided into those that previously failed, those that have arcuate cracks, and those that have not yet cracked or

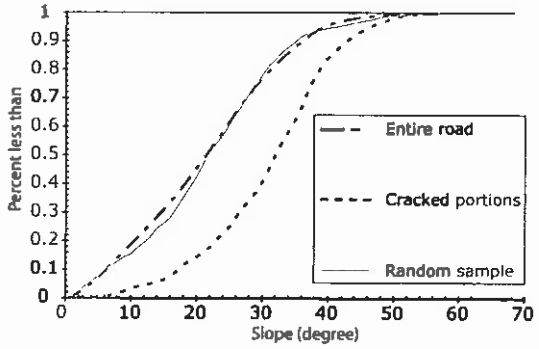

Figure 7. Plot shows a cumulative, normalized distribution of lumped failed-or-cracked slopes and the entire uncracked road. The distribution of 21 randomly selected, uncracked sites shows good agreement with the entire uncracked population.

Table 1. *Summary statistics for slope analysis.*

Slope Distribution	Mean	Median	Standard Deviation	N (sites)	N (cells)	Standard Error	Standard Error of Difference
Uncracked (lumped)	21.9	22	11.1	—	126,035	0.03	0.29
Failed-cracked (lumped)	31.6	33	9.86	—	1,166	0.33	0.29
Uncracked-random (site medians)	22.9	22	9.2	21	56 per site	2.01	2.42
Failed-cracked (site medians)	32.6	33	6.16	21	56 per site	1.34	2.42

failed but are topographically similar to the cracked and failed sites. For the purposes of the DEM analysis we treat the failed and cracked sites as equivalent, because cracking was observed prior to failure at all but one of the six failed sites and because we assume cracking indicates progressive failure, which may lead to catastrophic road collapse, as happened at the failed sites. Additionally, in developing the predictive model, we treat all uncracked portions of the roadway as part of the population of stable sites. After analyzing the distributions of the uncracked and failed-or-cracked sites, we discuss what fraction of the stable sites might actually belong to the potentially unstable population.

Although the lumped cracked-or-failed and uncracked distributions cover nearly the same range in slope values, they are distinctly different from one another. This is shown by a *t*-test comparing the mean slope for each population, 31.6° for the failed-or-cracked sites and 21.9° for the uncracked portion of the roadway. The means are significantly different at a confidence level greater than 99.99 percent ($P < 0.0001$; statistics for *t*-test are listed in Table 1). This result confirms our assumption that the failed-or-cracked sites can be clearly distinguished from the uncracked sites across this landscape.

The goal of the probabilistic model is to identify potentially unstable sites that have not yet developed cracks. The basic question is as follows: for a given site along the roadway, is the distribution of slopes within that site buffer more consistent with the failed-or-cracked slope distribution than with the uncracked distribution? If so, then that site may have an elevated probability of developing cracks and progressive or sudden failure in the future. The lumped slope distributions shown in Figures 5 through 7 cannot be used directly for this; rather, we must use the statistics for sets of individual sites.

We analyzed the slope distributions within each of the 21 individual failed-or-cracked sites and focused on the median slope within each site buffer, as representative of the overall steepness of the site. The median is a better central tendency measure because of the skew of the slope distributions. We also randomly selected 21 sites from the uncracked portion of the roadway and calculated the median slope from each slope distribution. The distributions of site-median slope for failed-or-cracked and uncracked sites are shown in Figure 8. Also shown are curves representing normal (Gaussian) probability density functions of site-median slope, $p(S)$, given by

$$p(S) = \frac{1}{\sqrt{2\pi}\sigma} \exp\left(-\frac{(S-\mu)^2}{2\sigma^2}\right) \qquad (1)$$

where μ and σ are the mean and standard deviation of the measured distributions, respectively. Figure 8 indicates that the distribution of possible site-median slopes can be treated as normally distributed, as predicted by the central limit theorem.

Like the lumped slope distributions in Figure 7, there is a clear difference in the site-median slopes between the failed-or-cracked and uncracked portions of the roadway. A *t*-test shows that the difference of 9.7° between the means of the site-median slopes is significant at a confidence level of 99 percent ($P < 0.01$; Table 1). We used the statistics of the site-median slope distributions to develop a model for evaluating the likelihood that any given currently uncracked site may be topographically more consis-

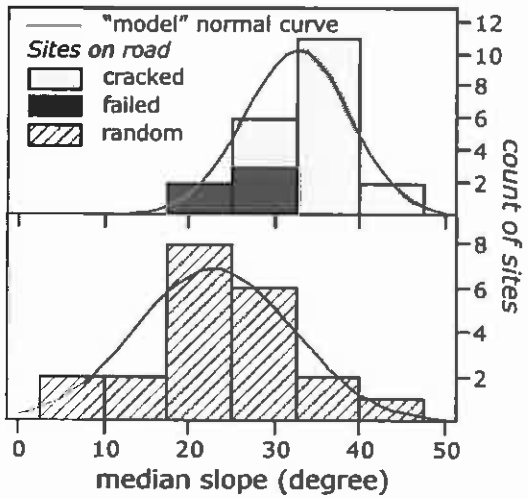

Figure 8. Frequency distribution plots of median slope from individual failed (N = 6) and cracked (N = 15) and randomly selected uncracked sites (N = 21). Model Gaussian (normal) curves are fitted to these distributions.

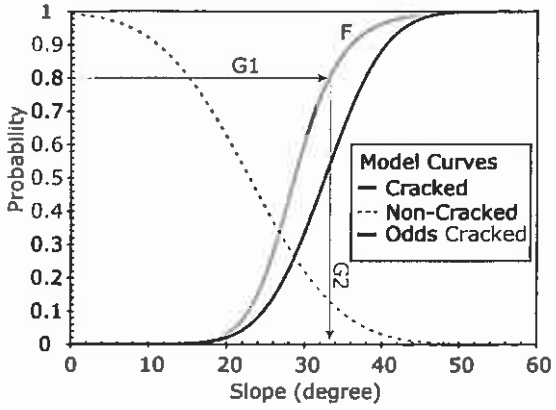

Figure 9. Diagram shows decision-making model used for determining the level of confidence (G1) and median slope, failure criterion (G2) associated with road-fill failure hazards. Curves are shown as cumulative, normalized distributions. See text for further explanation.

tent with the failed-or-cracked sites than with the population of uncracked sites.

Figure 9 shows the cumulative distribution, $P_c(S)$, for the normal fit to the failed-or-cracked site-median slopes, given by

$$P(S) = \int_0^S p(s)\hat{c}s \tag{2}$$

which describes the probability that any location that belongs to the population of potentially unstable sites will have a median slope less than or equal to S. Also plotted in Figure 9 is the complementary cumulative distribution, $P_u^*(S) = 1 - P_u(S)$, which describes the probability that a site will have a median slope greater than or equal to S if it belongs to the stable, uncracked site population. (Note that the subscripts "c" and "u" refer to the failed-or-cracked and uncracked distributions, respectively; the superscripted asterisk indicates the complementary cumulative distribution.) Figure 9 shows that as site-median slope increases, the value of $P_u^*(S)$ declines and the value of $P_c(S)$ increases, because steeper slopes are more likely to be unstable. Note that the two curves cross where the median slope equals ~29°.

Probabilistically, any currently uncracked site could be considered more consistent with the stable uncracked distribution if the median slope S is less than 29° and more consistent with the failed-or-cracked distribution for an S value of greater than 29°. To quantify the odds (O_c) that a given site-median slope S is more appropriately considered to be part of the failed-or-cracked distribution, we use the expression

$$O_c = \frac{P_c(S)}{P_c(S) + P_u^*(S)} \tag{3}$$

where the sum $P_c(S) + P_u^*(S)$ encompasses all possible outcomes. Eq. 3 states that O_c is the fraction of all outcomes represented by the probability that a site should be considered part of the cracked-or-failed distribution; O_c is thus constrained to vary between 0 and 1. For example, at $S = 29°$, where the two curves cross, $P_c(S) = 0.26 = P_u^*(S)$, so $P_c(S) + P_u^*(S) = 0.52$ and $O_s = 0.5$, are equivalent to "50-50" odds that the given site-median slope should be considered part of the potentially unstable population.

MODEL APPLICATION AND DISCUSSION

Our topographically based, field-calibrated, probabilistic approach gives land managers a tool for assessing the probability of road-fill failure using readily available topographic and road condition data. Application of the model requires that managers decide what confidence level is appropriate for determining the threshold site-median slope, above which sites would be classified as potentially unstable. In principle, the confidence level quantifies the willingness to accept the risk of a false-positive determination, which in this case is equivalent to declaring a site to be potentially hazardous when in fact it is more appropriately considered part of the population of sites with stable slopes. In our model, confidence level is numerically equal to O_c, as calculated in Eq. 3. Higher confidence levels and lower risk of false-positive determinations correspond to higher threshold slopes. Conversely, higher confidence levels also correspond to increased risk of a false-negative determination, which in this case would mean declaring a site to be stable when in fact it is more appropriately considered part of the population of potentially unstable sites. Selecting the correct confidence level to use requires consideration of the potential consequences of both false-positive and false-negative determinations.

Application of the decision model is illustrated in the following example, in which a confidence level of 80 percent has been selected. Figure 10 shows a conceptual model of the median-slope method and probabilistic hazard assessment. Figure 9 shows the analytical pathway (labeled G1) from the probability axis to the odds curve (labeled F) and the pathway (labeled G2) to the corresponding median-site slope above which sites would be considered potentially unstable, which here equals 33°. With 80 percent confidence, sites with median slopes steeper than 33° could be classified as potentially unstable, even though no pavement crack-

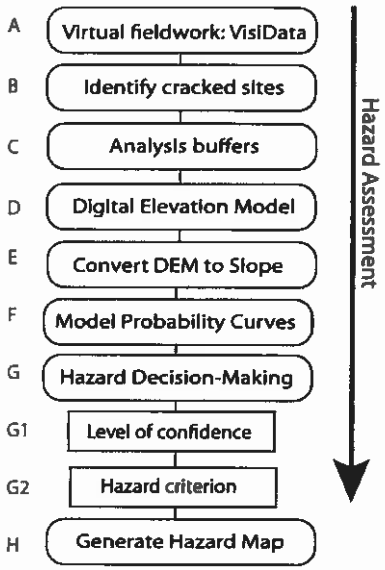

Figure 10. Conceptual model of hazard assessment using median-slope method and probabilistic assessment.

ing is currently evident. However, more than 50 percent of the potential sites assumed to belong to the failed-or-cracked population have median slopes of less than 33°. These sites present potential false-negative determinations when the confidence level is set at 80 percent. Figure 9 also shows that 14 percent of the sites assumed to belong to the stable, uncracked population have site-median slopes greater than 33° and thus would be classified as potentially unstable, a potential false-positive determination.

In practice, land managers would need to weigh the relative consequences of selecting high or low confidence levels in the context of the hazard assessment goals and priorities. The probabilistic model could be used in a number of distinct ways, including the following: (1) for prioritizing which road segments to study in more detail, in the field and with more deterministic modeling; (2) as a guide for establishing multiple levels of hazard classification; (3) to provide the public with a scientific basis for road closure during heavy rains; and (4) to determine whether other tools or data sets would further benefit the hazard assessment.

Other models could be used for more detailed analysis of potentially unstable sites identified by the median-slope method, such as SHALSTAB (Dietrich et al., 1995, 2001; Guimaraes et al., 2003). SHALSTAB uses shallow subsurface flow and hydrologic steady state with an infinite slope force balance to calculate a stability index that is equivalent to the ratio of rainfall intensity to soil strength properties (Dietrich et al., 1995). We implemented SHALSTAB on our study area and found that sites with steep median slopes are also generally less stable according to SHALSTAB. Figure 11 shows a portion of the roadway that was analyzed using our analytical model coded in Python and employing ArcGIS geoprocessing tools. The proportional symbols shown as circles represent ranges of median-slope classes. These symbols are shown over the output from the SHALSTAB model with the associated stability index. The correlation between higher median slopes from our model and increasingly unstable slopes from SHALSTAB is apparent. We were unable to extract distributions of stability index results to use in the buffer analysis approach used for the median-slope method, although this would be a useful comparison for future work.

The result that the lowest median slope values came from the failed sites was not expected (Figure 8). However, the proximity of these locations to the highest elevations and steepest slopes of Mount Mitchell indicates that rainfall intensity and duration were greater as a result of orographic forcing. This is not necessarily inconsistent with the site-median slope method, because we assume that potentially unstable sites become unstable when rainfall sufficient to initiate landsliding reaches the road fill.

Finally, we do not advocate our method as a substitute for on-foot evaluation of potential hazards nor as a complete model for assessing hazards. We view our method as a potentially useful new tool that uses existing data sets and technologies and provides a simple conceptual approach accessible to land managers with little hazard evaluation experience.

CONCLUSIONS

Road-fill failures pose a threat to human life, release sediment into watersheds, and are costly to repair. We developed a median-slope method and a probabilistic approach to predict road-fill failures along a portion of the Blue Ridge Parkway in North Carolina. We determined the distributions of slopes related to road-fill failure by mapping the locations of previous road-fill failures and sites of pavement arcuate cracks using virtual fieldwork and field verification. The slope distributions of failed-or-cracked sites and uncracked sites extracted within a 30-m–radius buffer from a LiDAR-derived DEM showed a statistically significant difference between the means of the medians of each distribution. Thus, the median slope value for any 30-m–radius section of road provided a criterion for delineating potential road-failure hazard. We developed a probabilistic decision model for land managers to (1) prioritize further study of particular road segments in the field; (2) classify multiple levels of hazard; (3) provide a scientific basis for road-closure;

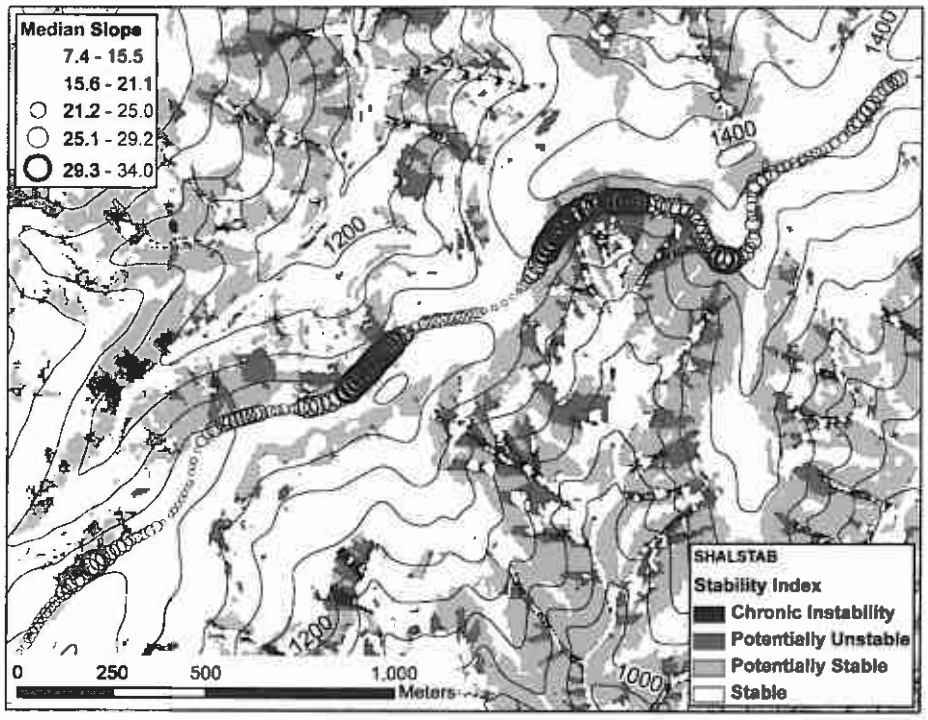

Figure 11. This segment of the Blue Ridge Parkway was analyzed using the median-slope hazard criterion compared to the SHALSTAB model, as described in the text. The circles are proportionally sized symbols representing five ranges of median slopes. Each symbol represents a range of median slopes from within a 30-m-radius analysis buffer. Bold circles represent hazards delineated with a 60–80 percent level of confidence. Refer to Figure 1 for location map.

and (4) determine whether other tools or data sets would further benefit the hazard assessment. Other GIS-based methods for analyzing road-related slope hazards, such as SHALSTAB, provide useful analyses that could help supplement a hazard assessment using the median-slope method.

ACKNOWLEDGMENTS

We thank the numerous federal and state personnel who provided significant assistance throughout this study, including Jim Amenta, J. David Anderson, Tom Collins, John Dixon, Paula Gori, Jackie Holt, Rebecca Latham, Susan Russell-Robinson, Bambi Teague, and Rick Wooten. Review comments from W. C. Haneberg, S. J. Prochnow, and T. R. West were of great assistance to the authors. We thank the U.S. Geological Survey and Sigma Xi: Grants-in-aid-of-research for funding portions of this project and the Geological Society of America for a student travel grant to R. J. Sas, Jr.

REFERENCES

Beven, J. L., II, 2004, *Tropical Cyclone Report Hurricane Frances, National Weather Service National Hurricane Center*: Electronic document, available at http://www.hpc.ncep.noaa.gov/tropical/rain/frances2004filledrainblk.gif

Collins, T. K., 2008, Debris flows caused by failure of fill slopes: Early detection, warning, and loss prevention: *Landslides*, Vol. 5, pp. 107–120.

Dietrich, W. E.; Bellugi, D.; and de Asua, R. R., 2001, Validation of the shallow landslide model, SHALSTAB, for forest management. In Wigmosta, M. S. and Burges, S. J. (Editors), *Land Use and Watersheds: Human Influence on Hydrology and Geomorphology in Urban and Forest Areas*: Water Science and Application, American Geophysical Union, Washington DC, Vol. 2, pp. 195–227.

Dietrich, W. E. and Montgomery, D. R., 1998, Hillslopes, channels and landscape scale. In Sposito, G. (Editor), *Scale Dependence and Scale Invariance in Hydrology*: Cambridge University Press, Cambridge, pp. 30–60.

Dietrich, W. E.; Reiss, R.; Hsu, M. L.; and Montgomery, D. R., 1995, A process-based model for colluvial soil depth and shallow landsliding using digital elevation data: *Hydrological Processes*, Vol. 9, pp. 383–400.

Douglas, I., 1967, Natural and man made erosion in the humid tropics of Australia, Malaysia, and Singapore: *International Association Scientific Hydrology*, Vol. 75, pp. 17–30.

Elliot, W. J. and Lewis, S. A., 2000, Linking the WEPP Model to stability models. In *Proceedings ASAE Annual International Meeting*: Paper 002150, St. Joseph, Minnesota.

Elliot, W. J. and Tysdal, L. M., 1999, Understanding and reducing erosion from insloping roads: *Journal Forestry*, Vol. 97, No. 8, pp. 30–34.

FEDERAL HIGHWAY ADMINISTRATION, 2004, Emergency Landslide Repair Blue Ridge Parkway, McDowell and Yancey County, North Carolina: Geotechnical Report 17-04, pp. 1–11.

FURNISS, M. J.; ROELOFS, T. D.; AND YEE, C. S., 1991, Road construction and maintenance, In Meehan, W. R. (Editor), *Influences of Forest and Rangeland Management on Salmonid Fishes and their Habitats*: American Fisheries Society Special Publication 19, pp. 297–324.

GUIMARAES, R. F.; MONTGOMERY, D. R.; GREENBERG, H. M.; FERNANDES, N. F.; TRANCOSO GOMES, R. A.; AND DE CARVALHO, O. A., 2003, Parameterization of soil properties for a model of topographic controls on shallow landsliding: Application to Rio de Janeiro: *Engineering Geology*, Vol. 69, pp. 99–108.

HANEBERG, W. C., 2004, A rational probabilistic method for spatially distributed landslide hazard assessment: *Environmental Engineering Geoscience*, Vol. 10, pp. 27–43.

LARSEN, M. C. AND PARKS, J. E., 1997, How wide is a road? The association of roads and mass-wasting in a forested montane environment: *Earth Surface Processes Landforms*, Vol. 22, pp. 835–848.

LATHAM, R. C., 2006, Slope stability along the North Carolina section of the Blue Ridge Parkway: *Geological Society America Abstracts Programs*, Vol. 38, p. 28.

MERSCHAT, C. E.; CATTANACH, B. L.; CARTER, M. W.; AND WIENER, L. S., 2006, Geology of the Mesoproterozoic basement and younger cover rocks in the west half of the Asheville 100,000 quadrangle, North Carolina and Tennessee: An updated look, In Labotka, T. C. and Hatcher, R. D., Jr. (Editors), *Geological Society of America, 2006 Southeastern Section Meeting: Field Trip Guidebook*, pp. 1–56.

NATIONAL CLIMATE DATA CENTER, 2000, *Asheville North Carolina Monthly Normals*: Electronic document, available at http://cirrus.dnr.state.sc.us/cgi-bin/sercc/cliMAIN.pl?nc0301

NORTH CAROLINA DEPARTMENT OF TRANSPORTATION, 2007, *LIDAR Contours and Elevation Data*: Electronic document, available at http://www.ncdot.org/it/gis/DataDistribution/ContourElevationData/default.html

NORTH CAROLINA GEOLOGICAL SURVEY, 1985, *Geologic Map of North Carolina*: North Carolina Geological Survey.

PACK, R. T.; TARBOTON, D. G.; AND GOODWIN, C. N., 1998, The SINMAP approach to terrain stability mapping: *Paper Submitted to 8th Congress of the International Association of Engineering Geology*: Vancouver, British Columbia, Canada, 21–25 September 1998.

STOCK, J. D. AND DIETRICH, W. E., 2006, Erosion of steepland valleys by debris flows: *Geological Society America Bulletin*, Vol. 118, pp. 1125–1148.

WEMPLE, B. C.; SWANSON, F. J.; AND JONES, J. A., 2001, Forest roads and geomorphic process interactions, Cascade Range, Oregon: *Earth Surface Processes Landforms*, Vol. 26, pp. 191–204.

WOOTEN, R. M.; GILLON, K. A.; WITT, A. C.; LATHAM, R. S.; DOUGLAS, T. J.; BAUER, J. B.; FUEMMELER, S. J.; AND LEE, L. G., 2008, Geologic, geomorphic, and meteorological aspects of debris flows triggered by Hurricanes Frances and Ivan during September 2004 in the Southern Appalachian Mountains of Macon County, North Carolina (southeastern USA): *Landslides*, Vol. 5, pp. 31–44.